
Learning Physics between Digital Twins with Low-Fidelity Models and Physics-Informed Gaussian Processes

Michail Spitieris^{1,2}, Ingelin Steinsland¹

¹Department of Mathematical Sciences

²Department of Public Health and Nursing

Norwegian University of Science and Technology (NTNU)

{michail.spitieris, ingelin.steinsland}@ntnu.no

Abstract

A digital twin is a computer model that represents an individual, for example a component, a patient or a process. In many situations we want to gain knowledge about an individual from its data while incorporating imperfect physical knowledge and also learn from data from other individuals. In this paper we introduce and demonstrate a fully Bayesian methodology for learning between digital twins in a setting where the physical parameters of each individual are of interest. For each individual the methodology is based on Bayesian calibration with model discrepancy. Through the discrepancy, modeled as a Gaussian process, the imperfect low-fidelity physical model is accounted for. Using ideas from Bayesian hierarchical models, a joint probabilistic model of digital twins is constructed by connecting them through a new level in the hierarchy. For the physical parameters the methodology can be seen as using a prior distribution in the individual model that is the posterior of the corresponding hyperparameter in the joint model. For learning the imperfect physics between individuals two approaches are introduced, one that assumes the same discrepancy for all individuals and one that can be seen as using a prior learned from all individuals for the parameters of the Gaussian processes representing the discrepancies. Based on recent advances related to physics informed priors, Hamiltonian Monte Carlo methods and using these for inverse problems we set up an inference methodology that allows our approach to be computational feasible also for physical models based on partial differential equations and individual data that are not aligned. The methodology is demonstrated in two synthetic case studies, a toy example previously used in the literature extended to more individuals and an example based on a cardiovascular differential equation model relevant for treatment of hypertension. The case studies show that 1) models not accounting for imperfect physical models are biased and over-confident, 2) the models accounting for imperfect physical models are more uncertain, but covers the truth, 3) the joint models have less uncertainty than the corresponding independent individual models, but are not over-confident.

1 Introduction

A definition of a digital twin is a virtual representation of a physical asset enabled through data and simulators [15]. Simulators refer to mathematical models and physical model based on first principles are often preferred both to incorporate system knowledge and to gain explainability. A known challenge of deployment of digital twins is scalability, i.e. the ability to accessible robust digital twin implementations at scale [15, 10].

The ability to make better decisions is the motivation for digital twins. In this paper, we consider the case that better decisions can be made with knowledge about the physical parameters of an imperfect physical model. In one of our case studies, a low fidelity model for the cardiovascular system, the Windkessel model [21] is used. This model is a differential equation linking blood flow and blood pressure and has two physically interpretable parameters that can direct the treatment of hypertension for patients. The parameters will vary between patients, and we aim to estimate these using noisy flow and pressure observations. It is known that low-fidelity models produce biased parameter estimates if we don't account for model discrepancy [5].

Recently, Spitieris and Steinsland [20] introduced and demonstrated a methodology for Bayesian analysis of imperfect physical models using physics informed Gaussian process priors. They combine a model formulation that accounts for discrepancy introduced by Kennedy and O'Hagan [11] with Physics-informed Gaussian process priors for physical models described by differential equations [14]. This gives computational efficiency and uncertainty quantification of the physical parameters of interest through a fully Bayesian approach.

For each digital twin accounting for model discrepancy combined with noisy data can result in too uncertain estimates to be of practical use. Further, there can be identification issues related to the discrepancy. The working hypothesis is that the uncertainty of the parameters for the individual digital twins can be reduced by using information from other digital twins. In this paper, we introduce a framework for how individual digital twins can share data to reduce uncertainty. The physical models are cast into a Bayesian hierarchical model framework which is extended with an extra level to allow both the physical parameters and the discrepancy to gain information from the other individuals. The code to replicate all the results in the paper is available at <https://github.com/MiSpitieris/Learning-Physics-between-DTs>.

2 Background

2.1 Accounting for model discrepancy

Let $\mathbf{x} = (x_1, \dots, x_k)$ be the k input variables, and $\phi = (\phi_1, \dots, \phi_p)$ the vector of unknown parameters for the physical model $\eta(\mathbf{x}, \phi)$. This model is typically a simplified representation of the reality \mathcal{R} , and does not fit the observed data well resulting in biased physical parameters ϕ estimates [5]. To account for this model form uncertainty, Kennedy and O'Hagan [11] (KOH) suggested a Bayesian calibration framework which incorporates a functional model discrepancy in the model formulation. More specifically, the noise corrupted observed data $\mathbf{y}^{\mathcal{R}}$ are described by the physical model η and the systematic model discrepancy δ as follows

$$y^{\mathcal{R}}(\mathbf{x}) = \eta(\mathbf{x}, \phi) + \delta(\mathbf{x}) + \varepsilon, \quad (1)$$

where ε is the noise term. Since the discrepancy is an unknown function of the inputs \mathbf{x} , KOH used a flexible Gaussian process prior [16] to model the discrepancy, $\delta(\mathbf{x}) \sim GP(0, K_\delta(\mathbf{x}, \mathbf{x}' | \boldsymbol{\omega}))$, where K_δ is the covariance function and $\boldsymbol{\omega}$ are kernel hyperparameters. The physical model is usually computational expensive and thus KOH replaced the physical model numerical simulator with an emulator which is a GP model trained on N simulator output runs trained on an experimental designed on the input and parameter space. This results to a GP model which utilizes the two sources of information, N simulator runs data and n observed data and has a computational complexity of $\mathcal{O}((N+n)^3)$, where typically $N \gg n$. If the deterministic model is fast to evaluate, the computational complexity reduces. If an i.i.d. Gaussian error term, $\varepsilon \sim N(0, \sigma^2)$ is assumed we get the following model formulation [8]

$$y^{\mathcal{R}} \sim GP(\eta(\mathbf{x}, \phi), K_\delta(\mathbf{x}, \mathbf{x}' | \boldsymbol{\omega}) + \sigma^2), \quad (2)$$

and this formulation will be used in Section 4. To infer model parameters $(\boldsymbol{\omega}, \phi, \sigma)$ in equation 2, Bayesian inference is used by assigning priors to the model unknowns and specifically priors that reflect underlying knowledge about ϕ , and the posterior distribution is sampled using MCMC.

2.2 Physics-informed (PI) priors

We focus on the construction of physics-informed Gaussian process priors for physical models that are described by linear differential equations $\mathcal{L}_x^\phi u(x) = f(x)$, where \mathcal{L} is the linear differential operator and ϕ the vector of physical parameters. To simplify the notation we take x to be univariate, however the following results apply to higher dimensions (e.g. see examples in [14, 20]).

Suppose we have observations of the functions u and f at potentially different locations x_{u1}, \dots, x_{un_u} and x_{f1}, \dots, x_{fn_f} , where n_u and n_f are the number of data for the functions u and f , respectively. The corresponding observed data are $\mathbf{y}_u = (y_{u1}, \dots, y_{un_u})$ and $\mathbf{y}_f = (y_{f1}, \dots, y_{fn_f})$. The observed data are functional and usually $u(x)$ is a smooth function. Thus it is often reasonable to assume a GP prior, $u(x) \sim GP(0, K_{uu}(x, x' | \boldsymbol{\theta}))$ to describe the $u(x)$. The derivative of a GP is also a GP [1] and more specifically $\text{Cov}\left(u(x), \frac{\partial u(x')}{\partial x'}\right) = \frac{\partial K_{uu}(x, x' | \boldsymbol{\theta})}{\partial x'}$ and $\text{Cov}\left(\frac{\partial u(x)}{\partial x}, \frac{\partial u(x')}{\partial x'}\right) = \frac{\partial^2 K_{uu}(x, x' | \boldsymbol{\theta})}{\partial x \partial x'}$, if the kernel is differentiable. Thus a convenient choice (but not the only) is the squared exponential kernel since it is infinitely differentiable.

Raissi et al. [14] utilized this result to build physics-informed priors for $\mathcal{L}_x^\phi u(x) = f(x)$ by assuming a GP prior on $u(x)$. Then we have that $f(t) \sim GP(0, K_{ff}(x, x' | \boldsymbol{\theta}, \boldsymbol{\phi}))$, where $K_{ff}(x, x' | \boldsymbol{\theta}, \boldsymbol{\phi}) = \mathcal{L}_x^\phi \mathcal{L}_{x'}^\phi K_{uu}(x, x' | \boldsymbol{\theta})$, and also $K_{uf}(x, x' | \boldsymbol{\theta}, \boldsymbol{\phi}) = \mathcal{L}_{x'}^\phi K_{uu}(x, x' | \boldsymbol{\theta})$ and $K_{fu}(x, x' | \boldsymbol{\theta}, \boldsymbol{\phi}) = \mathcal{L}_x^\phi K_{uu}(x, x' | \boldsymbol{\theta})$. This results in a multi-output (of u and f) GP model that satisfies the differential equation. It is also convenient that the physical parameters $\boldsymbol{\phi}$ have become hyperparameters of the physics-inspired covariance matrix and therefore standard tools for inference can be used, where Raissi et al. [14] used maximum likelihood and obtained point estimates.

This approach has been extended in a Bayesian framework [20] which also accounts for model discrepancy in a model formulation similar to equation 1. More specifically, for noise corrupted data y_u and y_f , we assume a discrepancy function on $u(x)$, and we have the following model formulation

$$\begin{aligned} y_u &= u(x_u) + \delta_u(x_u) + \varepsilon_u, \text{ where } \delta_u(x) \sim GP(0, K_\delta(x, x' | \boldsymbol{\omega})) \\ y_f &= f(x_f) + \varepsilon_f, \end{aligned}$$

where $\varepsilon_u \sim N(0, \sigma_u^2)$ and $\varepsilon_f \sim N(0, \sigma_f^2)$ are the error terms. By assuming that $u(x) \sim GP(\mu_u(x_u | \boldsymbol{\beta}), K_{uu}(x, x' | \boldsymbol{\theta}))$, where μ_u is a mean function with parameters $\boldsymbol{\beta}$, and consequently $\mu_f(x_f | \boldsymbol{\beta}, \boldsymbol{\phi}) = \mathcal{L}_x^\phi \mu_u(x_u | \boldsymbol{\beta})$ we get the following multi-output GP that accounts for model discrepancy

$$p(\mathbf{y} | \boldsymbol{\beta}, \boldsymbol{\theta}, \boldsymbol{\omega}, \boldsymbol{\phi}, \sigma_u, \sigma_f) = \mathcal{N}(\boldsymbol{\mu}, \mathbf{K}_{\text{disc}} + \mathbf{S}) \quad (3)$$

where $\mathbf{y} = \begin{bmatrix} \mathbf{y}_u \\ \mathbf{y}_f \end{bmatrix}$, $\mathbf{K}_{\text{disc}} = \begin{bmatrix} K_{uu}(\mathbf{X}_u, \mathbf{X}_u | \boldsymbol{\theta}) + K_\delta(\mathbf{X}_u, \mathbf{X}_u | \boldsymbol{\omega}) & K_{uf}(\mathbf{X}_u, \mathbf{X}_f | \boldsymbol{\theta}, \boldsymbol{\phi}) \\ K_{fu}(\mathbf{X}_f, \mathbf{X}_u | \boldsymbol{\theta}, \boldsymbol{\phi}) & K_{ff}(\mathbf{X}_f, \mathbf{X}_f | \boldsymbol{\theta}, \boldsymbol{\phi}) \end{bmatrix}$, $\mathbf{S} = \begin{bmatrix} \sigma_u^2 I_u & 0 \\ 0 & \sigma_f^2 I_f \end{bmatrix}$ and $\boldsymbol{\mu} = \begin{bmatrix} \mu_u(\mathbf{X}_u | \boldsymbol{\beta}) \\ \mu_f(\mathbf{X}_f | \boldsymbol{\beta}, \boldsymbol{\phi}) \end{bmatrix}$. Finally, to infer model hyperparameters Hamiltonian Monte Carlo (HMC) [12] is used and more specifically the NUTS variation [9].

For the rest of this paper we denote $\mathbf{X} = (\mathbf{X}_u, \mathbf{X}_f)$, where \mathbf{X} can be multivariate and eq. (3) can be written as $p(\mathbf{y} | \boldsymbol{\beta}, \boldsymbol{\theta}, \boldsymbol{\omega}, \boldsymbol{\phi}, \sigma_u, \sigma_f) = \mathcal{N}(\boldsymbol{\mu}(\mathbf{X} | \boldsymbol{\beta}, \boldsymbol{\phi}), \mathbf{K}_{\text{disc}}(\mathbf{X}, \mathbf{X} | \boldsymbol{\theta}, \boldsymbol{\omega}, \boldsymbol{\phi}, \sigma_u, \sigma_f) + \mathbf{S})$.

3 Hierarchical physical models accounting for model discrepancy

In this section, the model and inference method for sharing information between individuals about parameters in physical models and discrepancy are introduced. We assume that we have data from M individuals, where $m = \{1, \dots, M\}$ denotes the individual id, and \mathbf{X}_m and \mathbf{y}_m the corresponding matrix of observed input data and vector output for individual m .

Note that in the case of physics informed priors, the vectors \mathbf{X}_m and \mathbf{y}_m are joint for both the part related to u and f for individual m as described in Section 2.2. Our aim is to infer the physical parameters for each individual, denoted $\boldsymbol{\phi}_m$.

3.1 Hierarchical physical model, shared global parameters

We now set up our most general hierarchical model where the individuals are connected through distributions of the conditional priors of the individual parameters. The model is illustrated in Figure 1 and mathematically formulated below:

$$\text{Individual likelihood:} \quad \mathbf{y}_m | \boldsymbol{\eta}_m, \boldsymbol{\delta}_m \sim P(\mathbf{y}_m | \boldsymbol{\eta}_m, \boldsymbol{\delta}_m) \quad (4)$$

$$\text{Individual latent field:} \quad [\boldsymbol{\eta}_m, \boldsymbol{\delta}_m] | \boldsymbol{\psi}_m \sim GP(\boldsymbol{\mu}_m, K_m | \boldsymbol{\zeta}_m) \quad (5)$$

$$\text{Individual parameter priors:} \quad \boldsymbol{\zeta}_m | \boldsymbol{\psi} \sim P(\boldsymbol{\zeta}_m | \boldsymbol{\psi}) \quad (6)$$

$$\text{Global parameters priors:} \quad \boldsymbol{\psi} \sim P(\boldsymbol{\psi}) \quad (7)$$

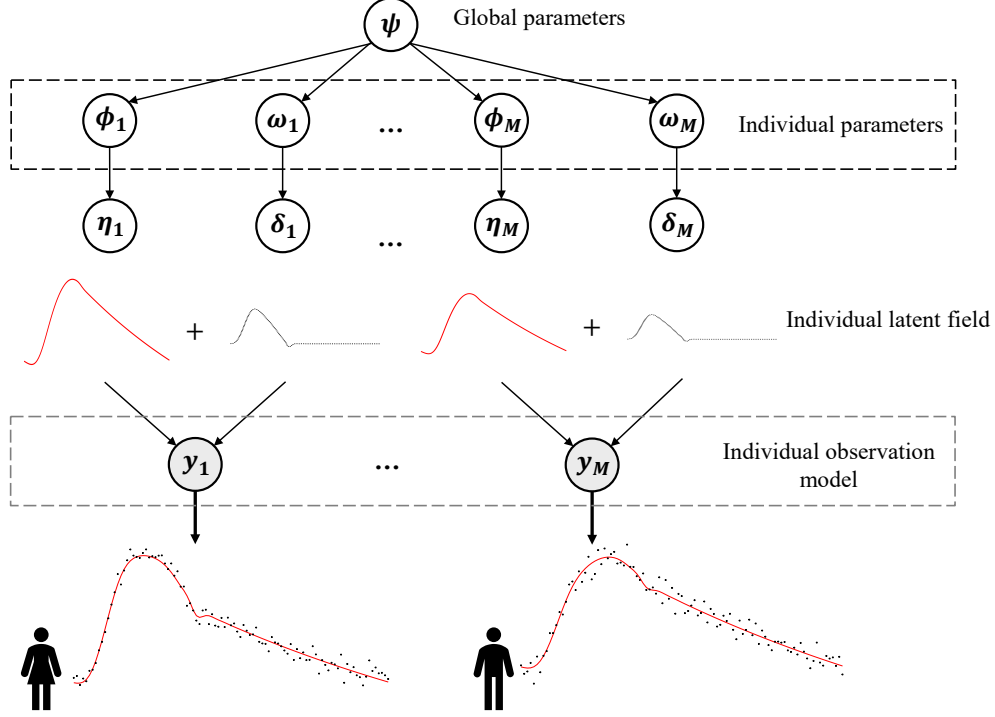


Figure 1: The hierarchical model detailed in Section 3 represented as directed acyclic graph (DAG). It presents the general case where the personalized physical model for the first and M -th individual is denoted as $\eta_1 = \eta(\mathbf{X}_1, \phi_1)$ and $\eta_M = \eta(\mathbf{X}_M, \phi_M)$ respectively and we are interested in learning the individual physical parameters ϕ_1, \dots, ϕ_M . In the individual latent field row, the red line represents the posterior mean of the (low fidelity) latent physical model and the black dashed line the posterior mean of the latent discrepancy model. At the bottom we have the posterior mean of the bias corrected (low fidelity) model, where the black dots are the observed data.

We start by describing the model component for each individual m , demonstrated for $m = 1$ and $m = M$ in Figure 1. Given the individual latent field $[\eta_m, \delta_m]$ the observations are assumed independent. There are possible parameters in the likelihood function, and we will use independent Gaussian noise $N(0, \sigma^2)$. The parameter σ^2 is suppressed from the notation in this section due to readability. The latent field consists of the physical model η_m and the discrepancy δ_m . Examples of these are given in Figure 1. We define $\mathbf{g}_m = [\eta_m, \delta_m]$. If we have a model formulated as in Equation 2 we have $\mathbf{g}_m \sim GP(\eta(\mathbf{X}_m, \phi_m), K_\delta(\mathbf{X}_m, \mathbf{X}_m | \omega_m))$ with K_δ and parameters as described in Section 2.1. If the PI prior formulation in Equation (3) is used we have $\mathbf{g}_m \sim GP(\mu(\mathbf{X}_m | \beta_m, \phi_m), \mathbf{K}_{\text{disc}}(\mathbf{X}_m, \mathbf{X}_m | \theta_m, \phi_m, \omega_m))$, with \mathbf{K}_{disc} and parameters as described in Section 2.2. The vector of all individual parameters for individual m are denoted ζ_m . If the model is formulated as in Equation 2 the vector ζ_m consists of the physical parameters ϕ_m and the discrepancy kernel hyperparameters ω_m , $\zeta_m = (\phi_m, \omega_m)$. When the physics informed priors formulation in Equations 3 is used the vector ζ_m in addition includes the kernel and mean parameters (θ_m, β_m) , and consequently $\zeta_m = (\phi_m, \theta_m, \beta_m, \omega_m)$.

The individual parameters are assumed to be conditionally independent given the global parameters ψ . Further, the global parameter is given a prior distribution. Hence, all these M individual models are connected through the global parameters.

Due to the conditional independence in the hierarchical model, the joint density of the model decomposes as follows

$$P(\mathbf{y}_1, \dots, \mathbf{y}_M, \mathbf{g}_1, \dots, \mathbf{g}_M, \zeta_1, \dots, \zeta_M, \psi) = P(\psi) \cdot \prod_{m=1}^M P(\mathbf{y}_m | \mathbf{g}_m) \cdot P(\mathbf{g}_m | \zeta_m) \cdot P(\zeta_m | \psi),$$

which means that the individual models are conditionally independent given the global parameters ψ .

3.2 Hierarchical physical model, common discrepancy and shared global parameters

In some cases the discrepancy can be (almost) similar for all individuals, and hence we want to assume common discrepancy parameters for all individuals. The m discrepancies are modeled as Gaussian processes with identical hyperparameters. This corresponds to $\delta_m(\mathbf{X}_m) \sim GP(0, K(\mathbf{X}_m, \mathbf{X}_m | \omega))$, with discrepancy hyperparameters $\omega_m = \omega$ that are identical for all the individuals.

3.3 Inference

Suppose that we have observations from M individuals where, $\mathbf{y}_{\text{pop}} = (\mathbf{y}_1, \dots, \mathbf{y}_M)$ and the corresponding inputs are $\mathbf{X}_{\text{pop}} = (\mathbf{X}_1, \dots, \mathbf{X}_M)$. The posterior distribution of the unknown parameters $\zeta = (\zeta_1, \dots, \zeta_M)$, $\mathbf{g} = (\mathbf{g}_1, \dots, \mathbf{g}_m)$, ψ and σ is given by the following equation

$$P(\mathbf{g}, \zeta, \psi | \mathbf{y}_{\text{pop}}, \mathbf{X}_{\text{pop}}) = P(\psi) \cdot \prod_{m=1}^M P(\mathbf{y}_m | \mathbf{g}_m, \mathbf{X}_m) \cdot P(\mathbf{g}_m | \zeta_m, \mathbf{X}_m) \cdot P(\zeta_m | \psi). \quad (8)$$

This posterior distribution is analytically intractable, and we rely on sampling methods. Since the dimension of the posterior is considerably large traditional MCMC methods, for example a Metropolis within Gibbs implementation can have slow mixing and fail to converge in practice. Hamiltonian Monte Carlo [12, 3] provides an efficient alternative for sampling high dimensional spaces (see for example [13]). The complex funnel-shape geometry of the posterior of hierarchical models can be hard to sample, while non-center parametrization can alleviate this problem [4] and it is used in this paper. More specifically, we use the NUTS [9] variation of HMC, implemented in the probabilistic language STAN [6].

If we assume for simplicity that each of the M individual has n observations, the computational complexity of the model is $\mathcal{O}(M \cdot n^3)$. Where the cubic complexity of the Gaussian process is scalable, since n is typically relatively small, and the complexity increases just linearly with the number of individuals M .

4 Toy example

We consider a conceptually simple model with one input parameter x and one physical parameter u which has been used in the literature [2]. The model represents the reality \mathcal{R} and the misspecified model, η are the following exponential models

$$\begin{aligned} y^R(x) &= 3.5 \cdot \exp(-u \cdot x) + b + \varepsilon \\ \eta(x, u) &= 5 \cdot \exp(-u \cdot x), \end{aligned}$$

where ε is a Gaussian noise term. For noise free data and for a given value of the physical parameter, $u = u_0$, the discrepancy between the two models is $-1.5 \cdot \exp(-u_0 \cdot x) + b$. However, we do not know the functional form in practice and thus assume a zero mean Gaussian process prior to describe the discrepancy function, $\delta(x) \sim GP(0, K_\delta(x, x' | \omega))$.

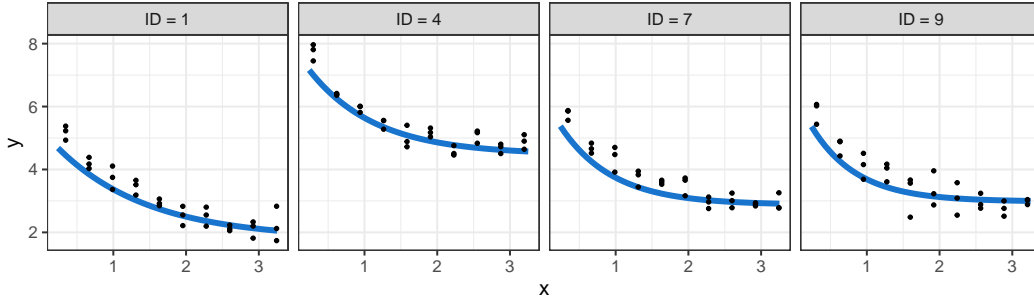


Figure 2: Toy example: Simulated noisy data for four of the ten individuals in the data set. The blue line is the true model ($5 \cdot \exp(-u_m \cdot x_m) + b_m$), and the dots are the corresponding noisy observed data y^R .

For the simulation study we assume there are $M = 10$ individuals. For each individual, data are simulated according to model $y^R(x)$. The true physical parameter u_m is set to be $0.7 + 0.1 \cdot m$, and hence $u_1 = 0.8$ and $u_{10} = 1.7$. The individual offsets b_m are sampled randomly from a uniform distribution on the interval $[0.5, 5]$. For all individuals $\varepsilon \sim N(0, 0.3^2)$. In Figure 2 the true model and simulated data are plotted for four individuals.

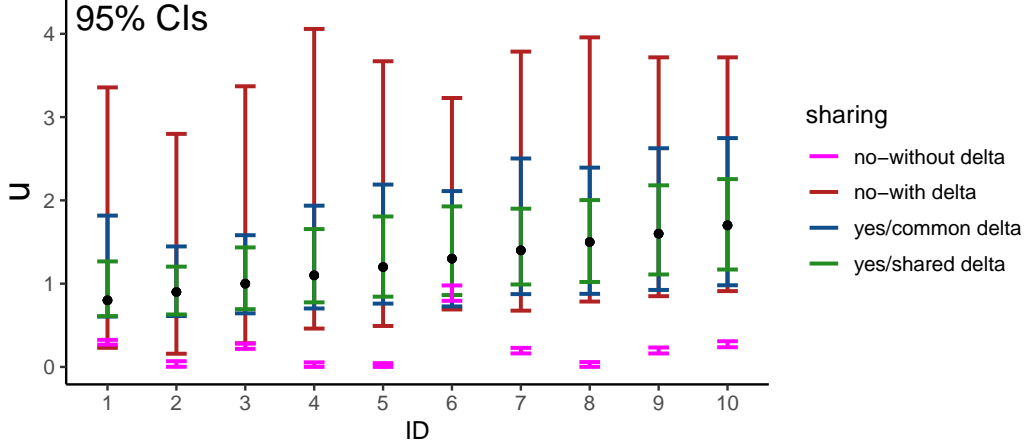


Figure 3: Toy example: 95% credibility intervals for the physical parameters based on posterior distributions for the four different models. The dots represent the true values of the parameter u_m for each of the individual.

We fit four different models to the simulated data. The first model (no-without delta in Figure 3), is the model η with Gaussian noise without assuming any model discrepancy, δ and therefore is the regression model $y(x) = 3.5 \cdot \exp(-u \cdot x) + \varepsilon$, where $\varepsilon \sim N(0, \sigma^2)$. The second model (no-with delta in Figure 3) accounts for model discrepancy and is given by equation 2. Both models do not share individual information and are fitted for each of the m participants independently. The third model (yes-common delta in Figure 3) shares information between individuals through a common discrepancy and inclusion of a global level parameter as described in Section 3.2. The fourth model (yes-shared delta in Figure 3) shares information between the individuals through global parameters for both the discrepancy and the physical parameters as described in Section 3.1. It allows the discrepancies to differ between individuals, δ_m and also share information through the parameters. Furthermore, for the models that account for discrepancy we assume that $\delta_m(x_m) \sim GP(0, K_\delta(x_m, x'_m))$, and we use the squared exponential kernel $K_\delta(x_m, x'_m) = \alpha_m^2 \exp\left(-\frac{(x_m - x'_m)^2}{2\rho_m^2}\right)$.

In Figure 3, we see the 95% credible intervals (CIs) of the physical parameter u_m for the four different model fits for each individual. First, we observe that if we do not account for model discrepancy (no-without delta) the model produces biased and over-confident parameter estimates which comes in line with Brynjarsdóttir and O’Hagan [5]. The posterior credible intervals (CIs) of the independent model which accounts for model discrepancy (no-with delta) cover the true values of the parameter. However, the uncertainties are quite large and this can be impractical for decision purposes. The posterior CIs of the models that share information (yes/common and shared delta), cover the true parameter value and they drastically reduce the posterior uncertainties. The model with individual discrepancies has the smallest uncertainties. This can be explained by its flexibility that allows individual discrepancies to share individual information between them without assuming a common discrepancy parameters. More information about the models, priors, predictions and implementation can be found in the Appendix.

5 Cardiovascular model example

5.1 Models

The Windkessel (WK) models [21] are linear differential equations that describe the relationship between the blood pressure, $P(t)$ and blood flow, $Q(t)$ in terms of physically interpretable parameters.

The two parameters WK model (WK2) is the basis for more complex models and is given by the following time-dependent linear differential equation

$$Q(t) = \frac{1}{R}P(t) + C\frac{dP(t)}{dt}, \quad (9)$$

where R is the total vascular resistance and C is the arterial compliance. These hemodynamical parameters are the physical parameters of interest. The three parameters WK model (WK3) is described by the following differential equation, $\frac{dP(t)}{dt} + \frac{P(t)}{R_2C} = \frac{Q(t)}{C} \left(1 + \frac{R_1}{R_2}\right) + R_1\frac{dQ(t)}{dt}$. The addition of the third parameter R_1 can increase model flexibility and might fit the observed data better, though it overestimates the total arterial compliance C [19]. In practice, R_1 controls the amplitude of the blood pressure waveform (see Figure 4) and therefore controls the discrepancy between the two models. The WK2 model is a special case of the WK3 when $R_1 = 0$ and also we have that $R^{\text{WK2}} = R_1^{\text{WK3}} + R_2^{\text{WK3}}$ [21], and this is an important connection for the simulation study in the following section.

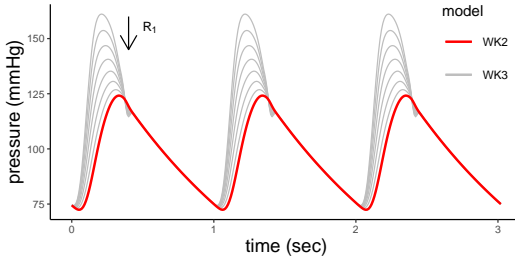


Figure 4: Blood pressure (three cardiac cycles/heart beats) generated from WK2 model (red) and for a range of range of R_1 values $[0.02, 0.12]$ from WK3 model (grey). The flow and C values are identical for both models. The amplitude of WK3-generated curve decreases linearly with R_1 , while the models become equivalent for $R_1 = 0$.

5.2 Simulation study

To validate our approach we need a model that is more complex than our modelling choice, but also with known connections between their physical parameters. Therefore, we use the WK2 model as a modelling choice, (η in Section 2.1) and simulate data from the WK3 model (see Figure 5), which we consider as the true model ($\mathbf{y}^{\mathcal{R}}$ in Section 2.1). We simulate data for $M = 9$ individuals. For each individual $m = 1, 2, \dots, 9$ we use an observed flow and given individual parameters R_{1m} , R_{2m} and C_m to simulate pressure observations. The individual parameters are chosen such that we have individuals with all the 9 possible combinations of the values $R_2 = (1, 1.15, 1.3)$ and $C = (0.95, 1.1, 1.25)$. The R_{1m} parameter which controls the discrepancy between WK2 and WK3 is sampled randomly from a uniform distribution on the interval $[0.02, 0.1]$. More specifically, for the blood flow $Q(t)$, we simulate the individual pressure $P_m(t) = \text{WK3}(Q(t), R_{1m}, R_{2m}, C_m)$, and we use \mathbf{t}_P temporal locations for the pressure observations and \mathbf{t}_Q temporal locations for the flow observations. The pressure observations and flow observations are not required to be aligned. We add i.i.d Gaussian noise to get flow and pressure observations as follows

$$\begin{aligned} \mathbf{y}_{P_m} &= P_m(\mathbf{t}_P) + \varepsilon_P, \varepsilon_P \sim N(0, 4^2) \\ \mathbf{y}_{Q_m} &= P_m(\mathbf{t}_Q) + \varepsilon_Q, \varepsilon_Q \sim N(0, 10^2). \end{aligned}$$

Our modelling choice, the WK2 model (9) is a linear differential equation which can be written as $\mathcal{L}_t^\phi P(t) = Q(x)$, where $\mathcal{L}_t^\phi = \frac{1}{R} + C\frac{d}{dt}$. By assuming that $P(t) \sim GP(\mu_P, K_{PP}(t, t' | \boldsymbol{\theta}))$, where $K_{PP}(t, t') = \alpha_{\text{WK2}}^2 \exp\left(-\frac{(t_P - t'_P)^2}{2\rho_{\text{WK2}}^2}\right)$, we construct a PI prior that accounts for model discrepancy as described in Section 2.2, given by the formulation (3) and we fit four different models as in the Section 4. The first model (no-without delta in Figure 6), is the PI prior without the model discrepancy, which is equivalent to model (3) but without the term K_δ in the first element of the covariance matrix. The second model (no-with delta in Figure 6) accounts for model discrepancy and is given by equation (3). Both models that do not share individual information and are fitted for each participant m independently. The third model (yes-common delta in Figure 6) shares information between individuals by assuming a common discrepancy and including global level parameters as described in Section 3.2. The fourth model (yes-shared delta in Figure 6) shares information between individuals through global parameters for both the model and physical parameters. For the models

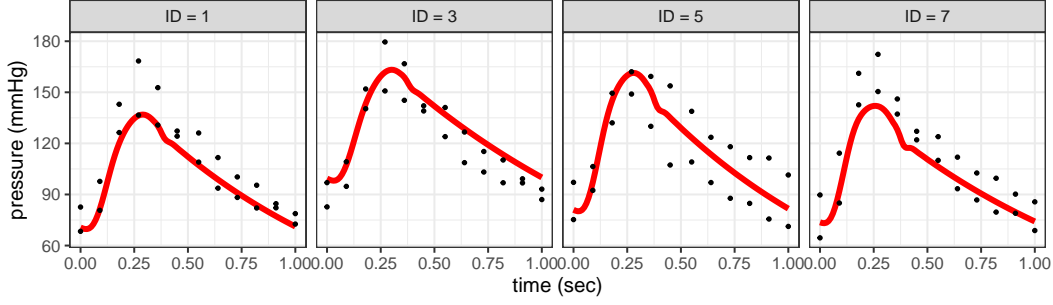


Figure 5: Cardiovascular simulation study: Simulated noisy pressure data for four of the nine individuals in the data set. The red line is the true model (WK3) and the dots are the observed blood pressure data.

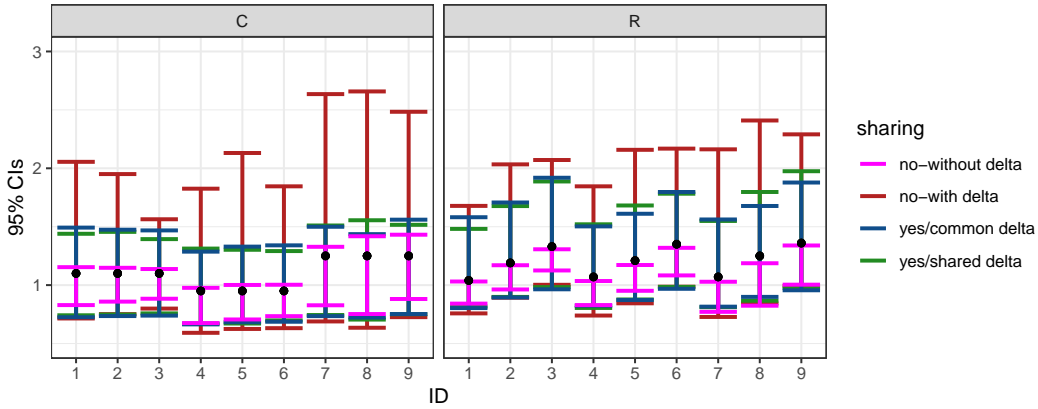


Figure 6: Cardiovascular simulation study: 95% credibility intervals for the physical parameters based on the posterior distributions for the four different models for each individual in the . The dots represent the true individual parameter values.

that account for discrepancy we assume that $\delta_m(t_P) \sim GP(0, K_{\delta_m}(t_P, t'_P))$, and we use the squared exponential kernel, $K_{\delta}(t_P, t'_P) = \alpha^2 \exp\left(-\frac{(t_P - t'_P)^2}{2\rho^2}\right)$.

In Figure 6, we see the 95% credible intervals for the posterior distributions of the physical parameters R_m and C_m , with the corresponding true values represented by the dots. Note, that the true R_m values are equal to $R_{1m} + R_{2m}$. First, we observe that the model which does not account for model discrepancy (no-without delta), systematically underestimates both physical parameters R and C which comes in line with [5] the results for the toy example in Section 4. For the C parameter the true value is within the 95% CI, though it is in the upper tail of the distribution. However, in practice the real observed data are different from the WK3 simulated data and the fit without accounting for discrepancy might result in larger biases. The independent models that account for model discrepancy (no-with delta), cover the true values for all individuals, though in some cases the uncertainty is quite large. For example, for the individuals 7-9 the posterior covers almost all the prior range, which is $R \sim Unif(0.5, 3)$, and thus the result can have low practical value. The models that share information between individuals (yes/common and shared delta) reduce the uncertainty substantially and still cover the true parameter values. However, compared to the toy example in Section 4, the model that shares discrepancy parameter information has similar performance to the model which assumes the same discrepancy for all individuals. This can be understood by observing that the discrepancies between the WK3 (true model) and the WK2 (modelling choice) are very similar, thus the correlation length scale and the marginal variance (ρ_m and α_m^2 parameters in K_{δ}), are similar for all individuals. Consequently, there is no need for considering different discrepancy parameters for each individual, and the more parsimonious parametrization of the model is sufficient. More details about the models, priors predictions and implementation can be found in the Appendix.

6 Discussion

We have presented a fully probabilistic modelling framework for learning physics between low fidelity physical models. To correct for model bias, we have included a functional discrepancy in the model formulation. The physical model and the model discrepancy have been incorporated in a Gaussian process prior, and our aim is to learn the physical parameters and account for their uncertainty. Therefore we introduced a Bayesian Hierarchical model where the individual physical and discrepancy parameters are connected through global parameters. We demonstrated our approach in two case studies, a toy example from the literature and a cardiovascular model where the hemodynamical parameters are of interest. We simulated data from a more complex model than our modelling choice, and we show that we can learn the physical parameters of the more complex model but also reduce the posterior uncertainty compared to fitting the models independently for each individual.

The proposed modelling framework is scalable since the computational complexity increases linearly with the number of individuals and is cubic for each individual, where usually the number of individual data is typically small. In cases where the individual data is large, GP methods for big data can be used (see e.g. [7, 18]). A known problem is the identifiability between the discrepancy and physical parameters in cases where prior information is vague. A remedy in this case is to express shape constraints in the discrepancy function through the derivative of the GP [5, 17].

References

- [1] R. J. Adler. *The geometry of random fields*. SIAM, 2010.
- [2] M. J. Bayarri, J. O. Berger, R. Paulo, J. Sacks, J. A. Cafeo, J. Cavendish, C.-H. Lin, and J. Tu. A framework for validation of computer models. *Technometrics*, 49(2):138–154, 2007.
- [3] M. Betancourt. A conceptual introduction to Hamiltonian Monte Carlo. *arXiv preprint arXiv:1701.02434*, 2017.
- [4] M. Betancourt and M. Girolami. Hamiltonian Monte Carlo for hierarchical models. *Current trends in Bayesian methodology with applications*, 79(30):2–4, 2015.
- [5] J. Brynjarsdóttir and A. O’Hagan. Learning about physical parameters: The importance of model discrepancy. *Inverse problems*, 30(11):114007, 2014.
- [6] B. Carpenter, A. Gelman, M. D. Hoffman, D. Lee, B. Goodrich, M. Betancourt, M. Brubaker, J. Guo, P. Li, and A. Riddell. Stan: A probabilistic programming language. *Journal of statistical software*, 76(1), 2017.
- [7] J. Hensman, A. G. Matthews, M. Filippone, and Z. Ghahramani. Mcmc for variationally sparse Gaussian processes. *Advances in Neural Information Processing Systems*, 28, 2015.
- [8] D. Higdon, M. Kennedy, J. C. Cavendish, J. A. Cafeo, and R. D. Ryne. Combining field data and computer simulations for calibration and prediction. *SIAM Journal on Scientific Computing*, 26(2):448–466, 2004.
- [9] M. D. Hoffman, A. Gelman, et al. The no-u-turn sampler: adaptively setting path lengths in Hamiltonian Monte Carlo. *J. Mach. Learn. Res.*, 15(1):1593–1623, 2014.
- [10] M. G. Kapteyn, J. V. Pretorius, and K. E. Willcox. A probabilistic graphical model foundation for enabling predictive digital twins at scale. *Nature Computational Science*, 1(5):337–347, 2021.
- [11] M. C. Kennedy and A. O’Hagan. Bayesian calibration of computer models. *Journal of the Royal Statistical Society: Series B (Statistical Methodology)*, 63(3):425–464, 2001.
- [12] R. M. Neal et al. Mcmc using Hamiltonian dynamics. *Handbook of markov chain monte carlo*, 2(11):2, 2011.
- [13] J. Piironen and A. Vehtari. Sparsity information and regularization in the horseshoe and other shrinkage priors. *Electronic Journal of Statistics*, 11(2):5018–5051, 2017.

- [14] M. Raissi, P. Perdikaris, and G. E. Karniadakis. Machine learning of linear differential equations using Gaussian processes. *Journal of Computational Physics*, 348:683–693, 2017.
- [15] A. Rasheed, O. San, and T. Kvamsdal. Digital twin: Values, challenges and enablers from a modeling perspective. *Ieee Access*, 8:21980–22012, 2020.
- [16] C. E. Rasmussen. Gaussian processes in machine learning. In *Summer School on Machine Learning*, pages 63–71. Springer, 2003.
- [17] J. Riihimäki and A. Vehtari. Gaussian processes with monotonicity information. In *Proceedings of the thirteenth international conference on artificial intelligence and statistics*, pages 645–652. JMLR Workshop and Conference Proceedings, 2010.
- [18] S. Rossi, M. Heinonen, E. Bonilla, Z. Shen, and M. Filippone. Sparse Gaussian processes revisited: Bayesian approaches to inducing-variable approximations. In *International Conference on Artificial Intelligence and Statistics*, pages 1837–1845. PMLR, 2021.
- [19] P. Segers, E. Rietzschel, M. De Buyzere, N. Stergiopoulos, N. Westerhof, L. Van Bortel, T. Gillebert, and P. Verdonck. Three-and four-element windkessel models: assessment of their fitting performance in a large cohort of healthy middle-aged individuals. *Proceedings of the Institution of Mechanical Engineers, Part H: Journal of Engineering in Medicine*, 222(4):417–428, 2008.
- [20] M. Spitieris and I. Steinsland. Bayesian calibration of imperfect computer models using physics-informed priors. *arXiv preprint arXiv:2201.06463*, 2022.
- [21] N. Westerhof, J.-W. Lankhaar, and B. E. Westerhof. The arterial windkessel. *Medical & biological engineering & computing*, 47(2):131–141, 2009.

Appendix

A Hierarchical physical model, common discrepancy and shared global parameters (Details on Section 3.2)

This is the case that inputs are observed at the same domain and discrepancy is expected to have similar characteristics. For example, in 1D and for the squared exponential kernel, $K_\delta(x_m, x'_m) = \alpha_m^2 \exp\left(-\frac{(x_m - x'_m)^2}{2\rho_m^2}\right)$ it means that the correlation decay characterized by ρ_m and the marginal variance α_m^2 is similar for all individuals, thus $\rho_m = \rho$ and $\alpha_m^2 = \alpha^2$ for $m = 1, \dots, M$. Therefore, ρ and α are not controlled by global parameters and their priors distributions have fixed parameter values.

For simplicity, let's consider the case that the physical model η is fast to evaluate and the input and the physical parameters are univariate and we have the following formulation $y^{\mathcal{R}}(x) = \eta(x, \phi) + \delta(x) + \varepsilon$. We follow the notation of Section 3.1 and for individual input data \mathbf{X}_m we have the latent field $\mathbf{g}_m \sim GP(\eta(\mathbf{X}_m, \phi_m), K_\delta(\mathbf{X}_m, \mathbf{X}_m | \boldsymbol{\omega}_m))$. In this case the vector of individual parameters $\boldsymbol{\zeta}_m$ consist of the individual physical parameter ϕ_m and the kernel hyperparameters $\boldsymbol{\omega}_m$, $\boldsymbol{\zeta}_m = (\phi_m, \boldsymbol{\omega}_m)$. In Section 3.1 both have priors $\phi_m \sim P(\phi_m | a_\phi, b_\phi)$, $\boldsymbol{\omega}_m \sim P(\boldsymbol{\omega}_m | \mathbf{a}_\omega, \mathbf{b}_\omega)$ that depend on the global parameters $a_\phi, b_\phi, \mathbf{a}_\omega, \mathbf{b}_\omega$, where $a_\phi \sim P(a_\phi)$, $b_\phi \sim P(b_\phi)$, $\mathbf{a}_\omega \sim P(\mathbf{a}_\omega)$ and $\mathbf{b}_\omega \sim P(\mathbf{b}_\omega)$. Now if we assume the same discrepancy across the individuals $m = 1, \dots, M$, we have again that $\phi_m \sim P(\phi_m | a_\phi, b_\phi)$, but $\mathbf{b} \sim P(\mathbf{b})$. More specifically if we use the squared exponential kernel for the discrepancy GP model, we have that $\boldsymbol{\omega} = (\rho, \alpha)$ and the joint density from Section 3.1 decomposes as follows

$$P(a_\phi)P(b_\phi) \cdot \prod_{m=1}^M P(\mathbf{y}_m | \mathbf{g}_m) \cdot P(\mathbf{g}_m | \phi_m, \rho, \alpha) \cdot P(\phi_m | a_\phi, b_\phi),$$

where $\rho \sim P(\rho)$, $\alpha \sim P(\alpha)$.

B Prior specification

In this Section we specify the non-center parameterization for the general case where the model is fast to evaluate and in the case of the PI GP prior.

B.1 General formulation: $y^{\mathcal{R}}(\mathbf{x}) = \eta(\mathbf{x}, \phi) + \delta(\mathbf{x}) + \varepsilon$

For simplicity, let's assume that the input x and the physical parameter ϕ are both univariate. We take a Gaussian prior on the physical parameter ϕ , $\phi \sim N(\mu_\phi, \sigma_\phi^2)$, and μ_ϕ, σ_ϕ are the global level parameters, where $\mu_\phi \sim P(\mu_\phi)$ and $\sigma_\phi \sim P(\sigma_\phi)$. Then we use the following non-center parameterization

$$\begin{aligned} \tilde{\nu}_\phi &\sim N(0, 1) \\ \phi &= \mu_\phi + \sigma_\phi \cdot \tilde{\nu}_\phi \sim N(\mu_\phi, \sigma_\phi^2). \end{aligned} \tag{10}$$

For the GP prior on the discrepancy $\delta(x) \sim GP(0, K_\delta(x, x' | \boldsymbol{\omega}))$, we use the squared-exponential kernel, $K_\delta(x, x') = \alpha^2 \exp\left(-\frac{(x - x')^2}{2\rho^2}\right)$ and $\boldsymbol{\omega} = (\alpha, \rho)$. For both parameters we use Log-normal priors. More specifically, $\rho \sim \text{Log-normal}(\mu_\rho, \sigma_\rho^2)$, where the distribution can be equivalently parameterized by the median m_ρ , $\rho \sim \text{Log-normal}(\log(m_\rho), \sigma_\rho^2)$. Then we use the following non-center parameterization

$$\begin{aligned} \tilde{\nu}_\rho &\sim N(0, 1) \\ \rho &= \exp(\log(m_\rho) + \sigma_\rho \cdot \tilde{\nu}_\rho) \sim \text{Log-normal}(\log(m_\rho), \sigma_\rho^2) \end{aligned} \tag{11}$$

and similarly for α we have that

$$\begin{aligned} \tilde{\nu}_\alpha &\sim N(0, 1) \\ \alpha &= \exp(\log(m_\alpha) + \sigma_\alpha \cdot \tilde{\nu}_\alpha) \sim \text{Log-normal}(\log(m_\alpha), \sigma_\alpha^2), \end{aligned} \tag{12}$$

where $m_\rho \sim P(m_\rho), \sigma_\rho \sim P(\sigma_\rho), m_\alpha \sim P(m_\alpha), \sigma_\alpha \sim P(\sigma_\alpha)$.

This can be generalized in cases where the physical parameters ϕ and inputs \mathbf{x} have higher dimension. Furthermore, the global level parameters the priors are chosen in a way that reflects the population level properties.

B.2 Physics-informed Gaussian process

The main difference when we use the PI GP prior compared to B.1, is that it involves the mean and kernel hyperparameters, (β, θ) in addition to the physical parameters ϕ . For the mean parameters, β we can use the same parameterization with the physical parameter ϕ as in B.1, while for the θ parameters we can use the same parameterization we used for the discrepancy kernel in B.1.

C Prediction equations

We provide prediction equations for the two modelling cases discussed in the paper. The first case is when the physical model $\eta(\mathbf{x}, \phi)$ is fast to run (e.g. a fast numerical solver). The second case is when we can use the physics-informed Gaussian process prior, and therefore no numerical discretization is needed.

C.1 General case

Standard GP predictions formulas can be used in this case, where the mean of the GP prior is the output of the physical model $\eta(\mathbf{x}, \phi)$ (eq. (2) in Section 2.1). More specifically, for the observed inputs \mathbf{X} , if $\mathbf{f} \sim GP(\eta(\mathbf{X}, \phi), K(\mathbf{X}, \mathbf{X}'))$, at new points \mathbf{X}_* the joint distribution of the noise corrupted data $\mathbf{y} = f(\mathbf{X}) + \varepsilon, \varepsilon \sim N(0, \sigma^2 I)$ and $f(\mathbf{X}_*) = \mathbf{f}_*$ is expressed as

$$\begin{bmatrix} \mathbf{y} \\ \mathbf{f}_* \end{bmatrix} \sim \mathcal{N} \left(\begin{bmatrix} \eta(\mathbf{X}, \phi) \\ \eta(\mathbf{X}_*, \phi) \end{bmatrix}, \begin{bmatrix} \mathbf{K} + \sigma^2 I & \mathbf{K}_* \\ \mathbf{K}_*^T & \mathbf{K}_{**} \end{bmatrix} \right), \quad (13)$$

where $\mathbf{K} = K(\mathbf{X}, \mathbf{X})$, $\mathbf{K}_* = K(\mathbf{X}, \mathbf{X}_*)$ and $\mathbf{K}_{**} = K(\mathbf{X}_*, \mathbf{X}_*)$. The conditional distribution of $p(\mathbf{f}_* | \mathbf{X}_*, \mathbf{X}, \mathbf{y})$ is also multivariate normal and more specifically

$$\begin{aligned} p(\mathbf{f}_* | \mathbf{X}_*, \mathbf{X}, \mathbf{y}) &= \mathcal{N}(\boldsymbol{\mu}_*, \boldsymbol{\Sigma}_*) \\ \text{where } \boldsymbol{\mu}_* &= \eta(\mathbf{X}_*, \phi) + \mathbf{K}_*^T (\mathbf{K} + \sigma^2 I)^{-1} (\mathbf{y} - \eta(\mathbf{X}, \phi)) \\ \text{and } \boldsymbol{\Sigma}_* &= \mathbf{K}_{**} - \mathbf{K}_*^T (\mathbf{K} + \sigma^2 I)^{-1} \mathbf{K}_*. \end{aligned} \quad (14)$$

C.2 Physics-informed Gaussian Process case

We present the prediction equations for the models formulated as PI GP priors in Section 3.1 and 3.2. Suppose want to predict both functional outputs, u and f at new inputs \mathbf{X}_u^* and \mathbf{X}_f^* respectively. Let $\mathbf{u}^* = u(\mathbf{X}_u^*)$ to be the predictions for u . The conditional distribution $p(\mathbf{u}^* | \mathbf{X}_u^*, \mathbf{X}, \mathbf{y}, \zeta)$ is multivariate Gaussian and more specifically

$$\begin{aligned} p(\mathbf{u}^* | \mathbf{X}_u^*, \mathbf{X}, \mathbf{y}, \zeta_\delta) &= \mathcal{N}(\boldsymbol{\mu}_u^*, \boldsymbol{\Sigma}_u^*) \\ \boldsymbol{\mu}_u^* &= \mu_u(\mathbf{X}_u^*) + \mathbf{V}_u^{*T} (\mathbf{K}_{\text{disc}} + \mathbf{S})^{-1} (\mathbf{y} - \boldsymbol{\mu}) \\ \boldsymbol{\Sigma}_u^* &= K_{uu}(\mathbf{X}_u^*, \mathbf{X}_u^*) + K_\delta(\mathbf{X}_u^*, \mathbf{X}_u^*) - \mathbf{V}_u^{*T} (\mathbf{K}_{\text{disc}} + \mathbf{S})^{-1} \mathbf{V}_u^*, \end{aligned} \quad (15)$$

where $\mathbf{V}_u^{*T} = [K_{uu}(\mathbf{X}_u^*, \mathbf{X}_u) \quad K_{uf}(\mathbf{X}_u^*, \mathbf{X}_f)]$. The conditional distribution $p(\mathbf{f}_* | \mathbf{X}_f^*, \mathbf{X}, \mathbf{y}, \zeta)$ is multivariate Gaussian and more specifically

$$\begin{aligned} p(\mathbf{f}_* | \mathbf{X}_f^*, \mathbf{X}, \mathbf{y}, \zeta_\delta) &= \mathcal{N}(\boldsymbol{\mu}_f^*, \boldsymbol{\Sigma}_f^*) \\ \boldsymbol{\mu}_f^* &= \mu_f(\mathbf{X}_f^*) + \mathbf{V}_f^{*T} (\mathbf{K}_{\text{disc}} + \mathbf{S})^{-1} (\mathbf{y} - \boldsymbol{\mu}) \\ \boldsymbol{\Sigma}_f^* &= K_{ff}(\mathbf{X}_f^*, \mathbf{X}_f^*) - \mathbf{V}_f^{*T} (\mathbf{K}_{\text{disc}} + \mathbf{S})^{-1} \mathbf{V}_f^*, \end{aligned} \quad (16)$$

where $\mathbf{V}_f^{*T} = [K_{fu}(\mathbf{X}_f^*, \mathbf{X}_u) \quad K_{ff}(\mathbf{X}_f^*, \mathbf{X}_f)]$.

D Toy example (Section 4)

In this Section additional results for the toy example in Section 4 are presented.

D.1 Posteriors for individual parameters

In Figure 7, we plot the posterior distributions for the physical parameter of interest u for all M individuals (ID) and the four different approaches. First, we observe that if we do not account for model discrepancy (no-without delta), the posterior distributions for all individuals are biased and do not cover the true value. The other three models which account for model discrepancy cover the true value; however, the model that does not share information (no-with delta) has too large uncertainty. In contrast, the other two models share information on the physical parameter with common discrepancy (yes/common delta) or shared information on the discrepancy (yes/ shared delta), reducing the posterior uncertainty. The latter is more flexible, allows for different discrepancies, and has the smallest uncertainty.

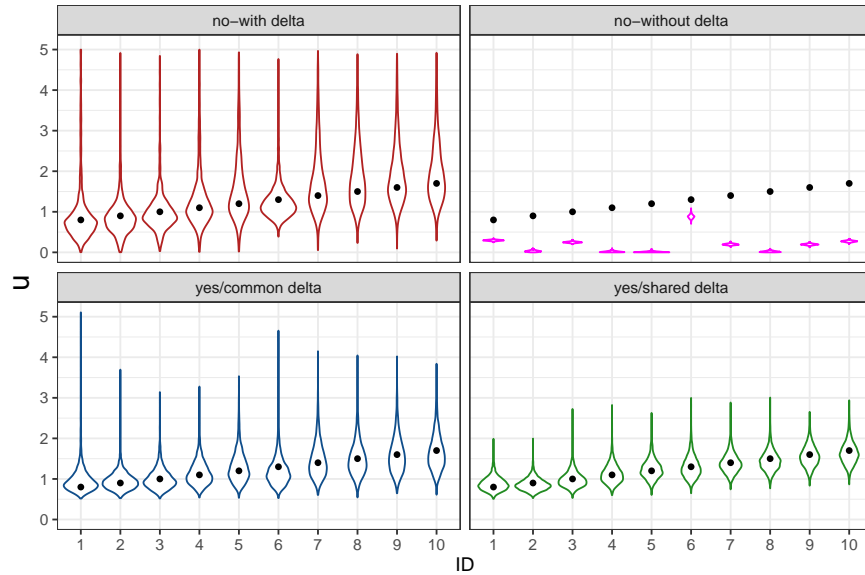


Figure 7: Toy example, posteriors.

D.2 Predictions

We now present the predictions obtained for all individuals as described in C. In Figure 8, we plot the predictions for all four approaches. We have two regions of predictions, on the left of the vertical dashed line where we have observed data (interpolation) and on the right where we have not observed data (extrapolation). First, we observe that the model which does not account for model discrepancy (no-without delta) does not fit the observed data well, and the prediction uncertainty is quite large. The other three approaches which account for model discrepancy perform similarly in the regions where we have observed data. While all three models perform well in regions without observed data, the model that shares information about both the physical parameter u and the discrepancy δ , has the smallest uncertainty.

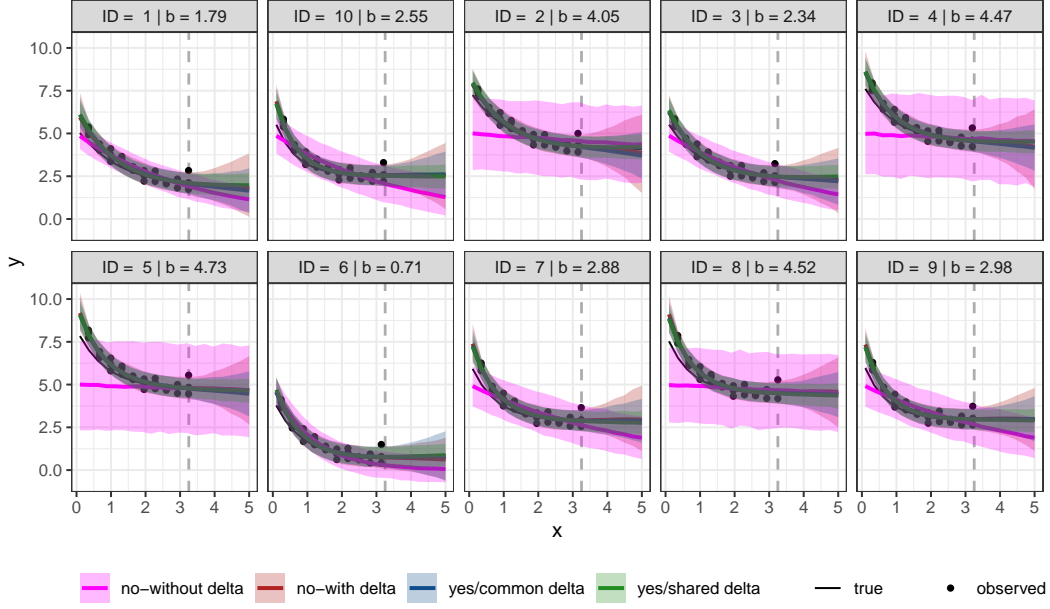


Figure 8: Toy example, predictions.

E Cardiovascular model (Section 5)

E.1 Physics-informed GP model

We provide details about the construction of the physics-informed prior WK model. The model is formulated as in Section 2.2, eq.(3) as follows

$$\begin{aligned} y_P &= P^{\text{WK}2}(t_P) + \delta(t_P) + \varepsilon_P \\ y_Q &= Q^{\text{WK}2}(t_Q) + \varepsilon_Q, \end{aligned} \quad (17)$$

where $P^{\text{WK}2}(t_P) \sim GP(\mu_P, K(t_P, t'_P))$, $\varepsilon_P \sim N(0, \sigma_P^2)$ and $\varepsilon_Q \sim N(0, \sigma_Q^2)$. In addition we assume a GP prior for the model discrepancy $\delta(t_P)$, $\delta(t_P) \sim GP(\mu_\delta, K_\delta(t_P, t'_P))$, resulting in the following multi-output GP prior

$$p(\mathbf{y} \mid \boldsymbol{\theta}, \phi, \sigma_P, \sigma_Q) = \mathcal{N}(\boldsymbol{\mu}, \mathbf{K}) \quad (18)$$

where

$$\begin{aligned} \mathbf{y} &= \begin{bmatrix} \mathbf{y}_P \\ \mathbf{y}_Q \end{bmatrix}, \\ \boldsymbol{\mu} &= \begin{bmatrix} \boldsymbol{\mu}_P \\ R^{-1} \cdot \boldsymbol{\mu}_P \end{bmatrix} \\ \mathbf{K} &= \begin{bmatrix} K_{PP}(\mathbf{t}_P, \mathbf{t}_P \mid \boldsymbol{\theta}) + K_\delta(\mathbf{t}_P, \mathbf{t}_P \mid \boldsymbol{\omega}) + \sigma_P^2 I_P & K_{PQ}(\mathbf{t}_P, \mathbf{t}_Q \mid \boldsymbol{\theta}, \phi) \\ K_{QP}(\mathbf{t}_Q, \mathbf{t}_P \mid \boldsymbol{\theta}, \phi) & K_{QQ}(\mathbf{t}_Q, \mathbf{t}_Q \mid \boldsymbol{\theta}, \phi) + \sigma_Q^2 I_Q \end{bmatrix} \end{aligned} \quad (19)$$

and

$$\begin{aligned} K_{PQ}(t, t') &= R^{-1} K_{PP}(t, t') + C \frac{\partial K_{PP}(t, t')}{\partial t'} \\ K_{QP}(t, t') &= R^{-1} K_{PP}(t, t') + C \frac{\partial K_{PP}(t, t')}{\partial t} \\ K_{QQ}(t, t') &= R^{-2} K_{PP}(t, t') + C^2 \frac{\partial^2 K_{PP}(t, t')}{\partial t \partial t'}. \end{aligned} \quad (20)$$

The PI GP model which does not account for model discrepancy is the same with the difference that from the first element of the covariance matrix \mathbf{K} , we remove the discrepancy kernel K_δ .

E.2 Posteriors for individual parameters R and C

In Figures 9 and 10, we plot the posterior distributions for R and C for all four approaches. In both Figures, we observe that for the model without discrepancy (no-without delta), the posteriors are over-confident and underestimate both R and C . The model which accounts for model discrepancy but does not share information (no-with delta) produces more reasonable estimates of the physical parameters, though in some cases, it can be too uncertain. For example, in Figure 10 the posterior can cover the whole range of possible values. The models that share information (yes/common delta and yes/shared delta) have reduced posterior uncertainty while covering the true values of R and C . Furthermore, posterior densities for the two models are very similar, suggesting that the more parsimonious model (yes/common discrepancy) is sufficient.

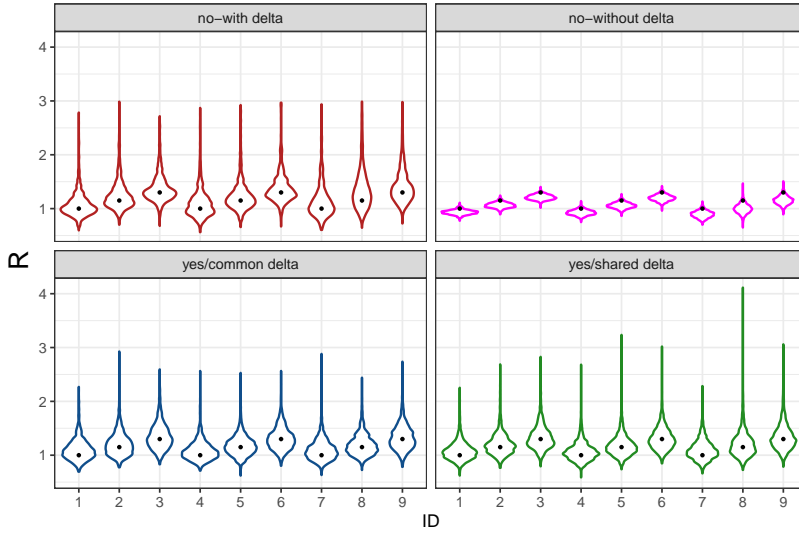


Figure 9: Cardiovascular model, posterior distribution, R .

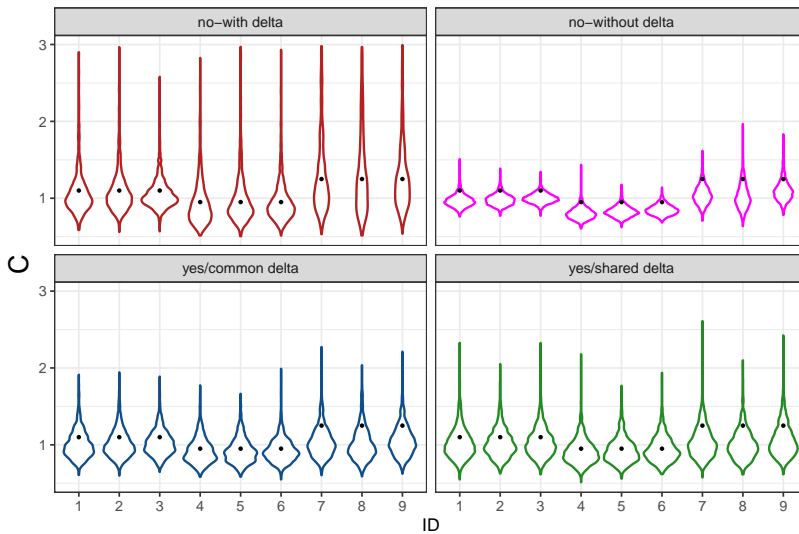


Figure 10: Cardiovascular model, posterior distribution, C .

E.3 Predictions

In Figures 11 and 12, the predictions for all four models for the two model outputs (blood pressure and blood flow) are plotted. The model which does not account for discrepancy produces more uncertain predictions than the other three models. We see that this uncertainty increases with the values of the parameter R_1 , which controls the discrepancy between the two models (WK2 and WK3). Even if the posterior uncertainty for R and C is larger for the model that does not share information (no-without delta), its prediction uncertainty is similar to the two models that share information (yes/common delta and yes/shared delta). In Figure 12, the blood flow predictions are plotted. All models perform similarly, but the model that does not account for discrepancy (no-without delta) has slightly larger prediction uncertainty.

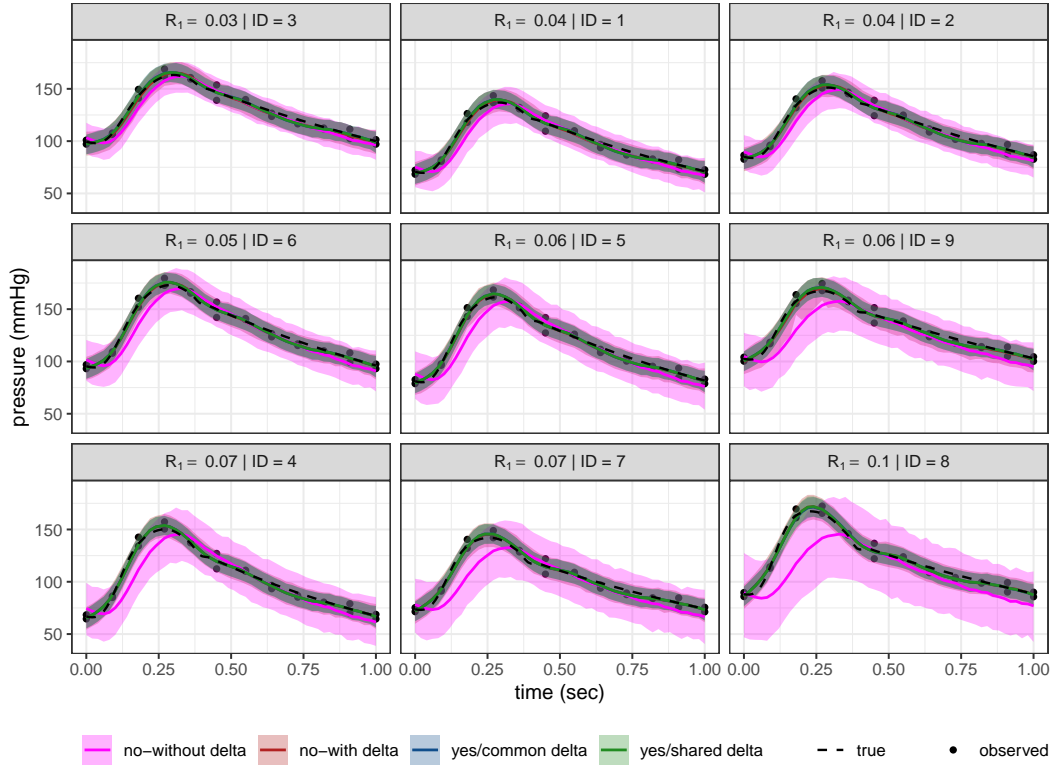


Figure 11: Cardiovascular model, pressure predictions.

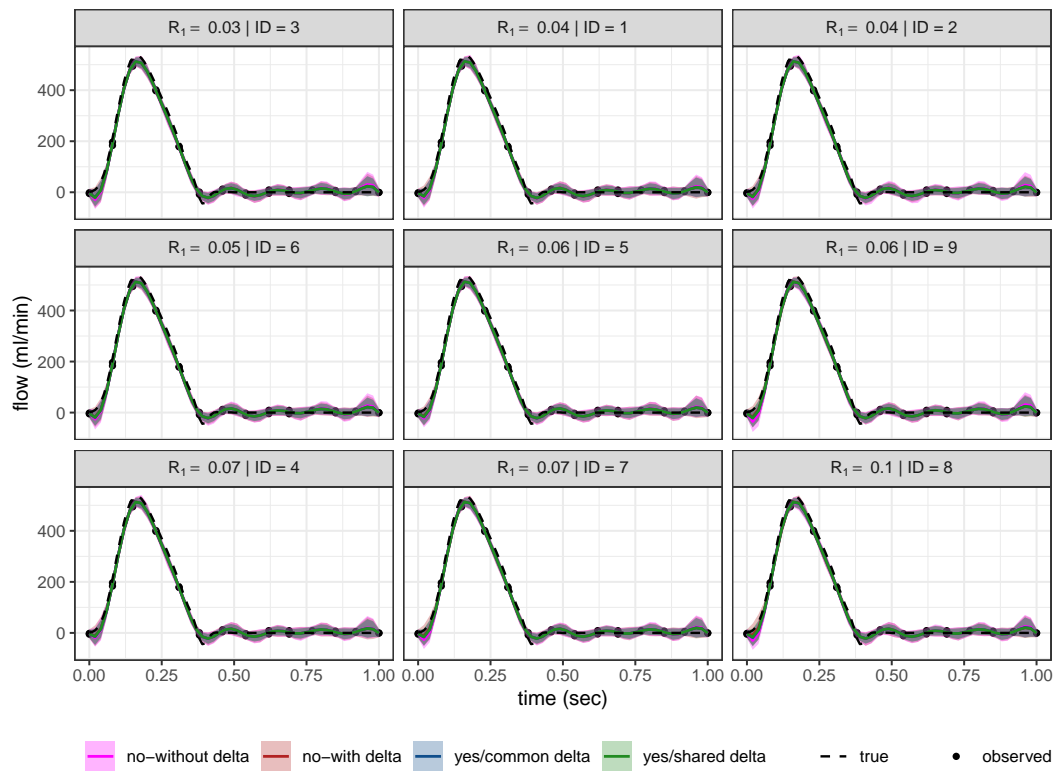


Figure 12: Cardiovascular model, flow predictions.